J Solid State Electrochem (2012) 16:759–766
DOI 10.1007/s10008-011-1430-8

ORIGINAL PAPER

One-pot synthesis of highly dispersed palladium nanoparticles on acetylenic ionic liquid polymer functionalized carbon nanotubes for electrocatalytic oxidation of glucose

Yinjie Kuang · Bohua Wu · Dan Hu · Xiaohua Zhang · Jinhua Chen

Received: 29 September 2010 / Revised: 20 March 2011 / Accepted: 4 May 2011 / Published online: 12 May 2011

Abstract A facile method for one-pot synthesis of highly dispersed palladium nanoparticles on acetylenic ionic liquid polymer functionalized carbon nanotubes (PdNPs-AILP-CNTs) has been developed in this paper. The nanohybrids are prepared by polymerization of acetylenic ionic liquid monomers catalyzed by $PdCl_2$, which is further reduced to PdNPs by $NaBH_4$ on CNTs in one pot and characterized by Fourier transform infrared spectroscopy, Raman spectroscopy, thermogravimetric analysis, and transmission electron microscopy. The electrocatalytic oxidation of glucose on the PdNPs-AILP-CNT nanohybrids is also investigated by cyclic voltammetry and chronoamperometry. The results show that the PdNPs with a particle size of around 3.5 nm disperse uniformly on CNTs, and PdNPs-AILP-CNT nanohybrids have good electrocatalytic performance for glucose oxidation.

Keywords One-pot synthesis · Palladium nanoparticles · Acetylenic ionic liquid polymer · Glucose electrooxidation

Electronic supplementary material The online version of this article (doi:10.1007/s10008-011-1430-8) contains supplementary material, which is available to authorized users.

Y. Kuang · B. Wu · D. Hu · X. Zhang · J. Chen (✉)
State Key Laboratory of Chemo/Biosensing and Chemometrics,
College of Chemistry and Chemical Engineering,
Hunan University,
Changsha 410082, People's Republic of China
e-mail: chenjinhua@hnu.cn

Y. Kuang
School of Chemistry and Biology Engineering,
Changsha University of Science & Technology,
Changsha 410114, People's Republic of China

Introduction

Palladium nanoparticles (PdNPs) have extensive applications in both heterogeneous and homogeneous catalytic reactions. They are one of the most efficient catalysts in the formation of carbon–carbon bonds, as well as in coupling reactions and chemical transformations such as hydrogenation and carbonylation [1]. Lately, Pd is attracting increasing interest as a promising electrocatalyst, replacing platinum (Pt) in alkaline alcohol fuel cells for the quicker oxidation kinetics of various alcohols such as ethanol, ethylene glycol, glycerol, and glucose [2]. Furthermore, the abundance of Pd on the earth is at least 50 times more than that of Pt.

On the other hand, owing to their large specific surface areas, high electrical conductivity, and chemical stability [3], carbon nanotubes (CNTs) have become one of the most significant materials in nanoscience and nanotechnology since their discovery. Recently, PdNP-CNT nanohybrids have been developed as advanced sensors and electrocatalysts in fuel cells [4–8]. However, it is still a challenge to anchor PdNPs on CNTs with high dispersion and small particle size. Several routes have been developed for the preparation of PdNP-CNT nanohybrids, including thermal decomposition [9], electroless deposition [10], microemulsion [11], chemical reduction in supercritical CO_2 solution [12], ethylene glycol reduction [13], surfactant self-reduction [14], and arc discharge in solution [15]. Although these routes are effective to anchor Pd nanoparticles on CNTs, they use either a complicated synthetic process or expensive equipment. Moreover, in most cases, the dispersion of PdNPs on CNTs is not usually satisfactory.

It was reported that imidazolium-based ionic liquids are excellent media for the preparation and stabilization of transition metal nanoparticles with a narrow size distribu-

tion [16]. Both the electrostatic and coordination effects of ionic liquids contribute to the stabilization of metal nanoparticles, and similar benefits may occur for ionic liquid polymers [17, 18]. A high-molecular-weight ionic liquid polymer should further endow a steric stabilization effect in addition to the effects mentioned above [19]. Ionic liquid polymers have been used to stabilize effectively Au, Pt, and Pd nanoparticles, as well as organizing nanoparticles into ordered structures with different topologies [19, 20]. Recently, we have prepared highly uniformly dispersed platinum nanoparticles on CNTs functionalized by 3-ethyl-1-vinylimidazolium ionic liquid polymers, and good electrocatalytic activity for methanol oxidation was observed [21]. However, till now, the ionic liquid polymers developed are electronically insulative, which is of no benefit to their applications in electrochemistry, especially in fuel cells. To solve this problem, conductive ionic liquid polymers may be a good alternative.

Herein, we report for the first time to functionalize CNTs with a conductive ionic liquid polymer (acetylenic ionic liquid polymer (AILP)) and developed a facile approach to prepare PdNPs on CNTs with both high dispersion and small particle size. The AILP layer was formed on the CNT surface by polymerization of acetylenic ionic liquid monomers catalyzed by palladium dichloride which was reduced and dispersed on CNTs in one pot. In this strategy, palladium dichloride is not only used as the catalyst for the formation of AILP but also as the precursor of PdNPs to synthesize PdNPs-AILP-CNT nanohybrids. Furthermore, the electrocatalytic performance of PdNPs-AILP-CNT nanohybrids for glucose oxidation was investigated by cyclic voltammetry and chronoamperometry because of their potential applications in fuel cells and biosensors.

Experimental section

Materials

Mutiwalled CNTs (length, 1–2 μm; diameter, 20–40 nm) were purchased from Shenzhen Nanotech Port Co. Ltd., China. 1-Methylimidazole (MI, 99%) and propargyl bromide (97%, 80% *w*/*w* in toluene) were purchased from Alfa Aesar. Except specific statement, chemicals were of analytical grade and used as received. *N*,*N*-dimethylformamide (DMF), dichloromethane, and diethyl ether were dried by 4 Å zeolite before use.

Synthesis of 1-methyl-3-(prop-2-ynyl)-imidazolium bromide

The procedure, with minor modification, for the synthesis of 1-methyl-3-(prop-2-ynyl)-imidazolium bromide [MPYI]Br is referred to in literature [22]. In brief, dichloromethane (10 mL), 1-methylimidazole (3.5 mL, 43.5 mmol), and 80% propargyl bromide in toluene (5 mL, 45 mmol) were stirred together for 4 h at room temperature. The mixture was washed by dichloromethane twice, and the solvent was removed by vacuum distillation. After thorough washing with diethyl ether (3×25 mL), the beige product (5.48 g, 62.7%) was dried in a vacuum oven at 323 K to remove residual solvent.

One-pot synthesis of poly(1-methyl-3-(prop-2-ynyl)-imidazolium bromide) functionalized CNTs and PdNPs-AILP-CNT nanohybrids

The synthesis procedure is that in the literature [23], used with some modification. In a typical run, a baked 25-mL two-neck flask equipped with condenser under an atmosphere of dry nitrogen was used, and 90 mg of 1-methyl-3-(prop-2-ynyl)-imidazolium bromide, 56 mg of $PdCl_2$, 60 mg of mutiwalled CNTs, and 6 mL of DMF were added. After being ultrasonicated for 15 min, the mixture was stirred and refluxed for 10 h at 383 K under nitrogen. The mixture was then diluted with double-distilled water after cooling to room temperature. Then, the pH value of the solution was adjusted to about 9 with ammonia and $NaBH_4$ dissolved in methanol (16 mL, 30 mM) was next added dropwise while vigorously stirring. The resulting solution was filtered, and the precipitate obtained was washed with methanol and double-distilled water several times to thoroughly remove adsorbed polymer, solvent, and unreacted ionic liquid monomer from the surface of CNTs. The final product, labeled as PdNPs-AILP-CNT nanohybrids, was then dried under vacuum at 323 K.

For comparison, PdNP-decorated CNTs (PdNPs-CNTs) were obtained by reducing the mixed solution of $PdCl_2$ and the CNTs with $NaBH_4$ methanol solution. In order to evaluate the electronic conductivity of the ionic liquid polymer film, AILP-functionalized CNTs (CNTs-AILP) were synthesized according to the above procedure except for the addition of $NaBH_4$. 1-Vinyl-3-ethyl imidazolium bromide ([VEIM]Br) polymer (non-conductive ionic liquid polymer) functionalized CNTs (CNTs-PIL) were prepared according to the procedure reported in the literature [24]. The brief procedure was as follows: 25 mg CNTs was added to 25.0 mL of methanol containing 5 mg [VEIM]Br and 1 mg 2,2'-azobisisobutyronitrile. The mixture was ultrasonicated for 15 min and then transferred to a 50-mL round-bottomed flask equipped with a condenser and magnetic stirrer, refluxed for 16 h at 353 K under vigorous stirring and N_2 protection. After cooling down, the mixture was filtered and washed with methanol and double-distilled water several times. The final product, labeled as CNT-PIL nanohybrids, was then dried under vacuum at 323 K.

Characterization

Proton nuclear magnetic resonance (^{1}H NMR) spectra were obtained at 20 °C with a Bruker DMX400 instrument with $SiMe_4$ as an external standard. Mass spectroscopy was performed on a LCQ Advantage instrument. Fourier transform infrared (FT-IR) spectra were recorded on a NICOLET 6700 FT-IR spectrometer. The thermal gravimetric analysis (TGA) was performed on a NETZSCH STA 409 PC at a heating rate of 10 °C min^{-1} under a nitrogen atmosphere. The morphology of the samples was characterized by transmission electron microscopy (TEM, TECNAI F20, FEI Company) with an accelerating voltage of 200 kV. The weight percent of Pd in the composites was investigated by inductively coupled plasma atomic emission spectroscopy and about 10.5 wt.% for PdNPs-AILP-CNTs (8.5 wt.% for PdNPs-CNTs).

The electrochemical properties of the samples were investigated by cyclic voltammetry and chronoamperometry, which were carried out on a CHI660B (Chenhua Instrument Company of Shanghai, China) electrochemical workstation with a conventional three-electrode glass cell. Pt wire and Ag/AgCl electrode were used as the counter and reference electrodes, respectively. The working electrode was generally prepared as follows: 2 mg of electrocatalyst sample was ultrasonically dispersed in 1 mL double-distilled water to form a homogeneous ink. A 20-μL catalyst ink was transferred by a microsyringe onto the surface of a cleaned glassy carbon (GC) electrode with the diameter of 5 mm. The loading mass of Pd was 21 μg cm^{-2} and 17 μg cm^{-2} for the PdNPs-AILP-CNTs and PdNP-CNT modified GC electrodes, respectively. After being dried in air, the electrode was coated with 5 μL of 0.5% Nafion ethanol solution. The electrocatalytic performance of the samples for the glucose oxidation was investigated in a 0.1-M KOH+50 mM glucose solution. The electrochemical impedance measurements were carried out with an IM6ex electrochemical analyzer system (ZAHNER Elektrik), and the electrode was prepared by dropping 10 μL aqueous solution of CNTs-AILP or CNTs-PIL (1 mg mL^{-1}) onto GC electrode and dried in air at room temperature. All electrochemical experiments were carried out at room temperature, and the potentials quoted in this paper are with respect to the Ag/AgCl electrode (saturated KCl solution).

Results and discussion

Synthesis of 1-methyl-3-(prop-2-ynyl)-imidazolium bromide, poly(1-methyl-3-(prop-2-ynyl)-imidazolium bromide) functionalized CNTs, and PdNPs-AILP-CNT nanohybrids

The synthesis of the 1-methyl-3-(prop-2-ynyl)-imidazolium bromide ([MPYI]Br) is shown in Fig. 1a. The structure of the product was evaluated by NMR and mass spectroscopy. The results are as follows: ^{1}H NMR (D_2O), δ=8.93 [1 H, s, N=CHN], 7.63 [1 H, t, NCH=CHN], 7.52 [1 H, t, NCH=CHN], 5.13 [2 H, s, $NCH{=}CHNCH_2$], 3.96 [3 H, s, NCH_3], 3.12 [1 H, s, C≡CH]; *m/z* (ESI, 5KV) 121 (M-Br, 100%) (See the electronic supplementary materials, Figs. S1 and S2). The results from ^{1}H NMR spectra and mass spectrum, which show that the molecular weight of [MPYI]Br is 201, demonstrate that the structure of [MPYI]Br is as expected, see Fig. 1a. On the other hand, the procedure for one-pot synthesis of PdNPs-AILP-CNT nanohybrids is shown in Fig. 1b. First, AILP-functionalized CNTs were prepared by in situ polymerization of [MPYI]Br monomer in DMF

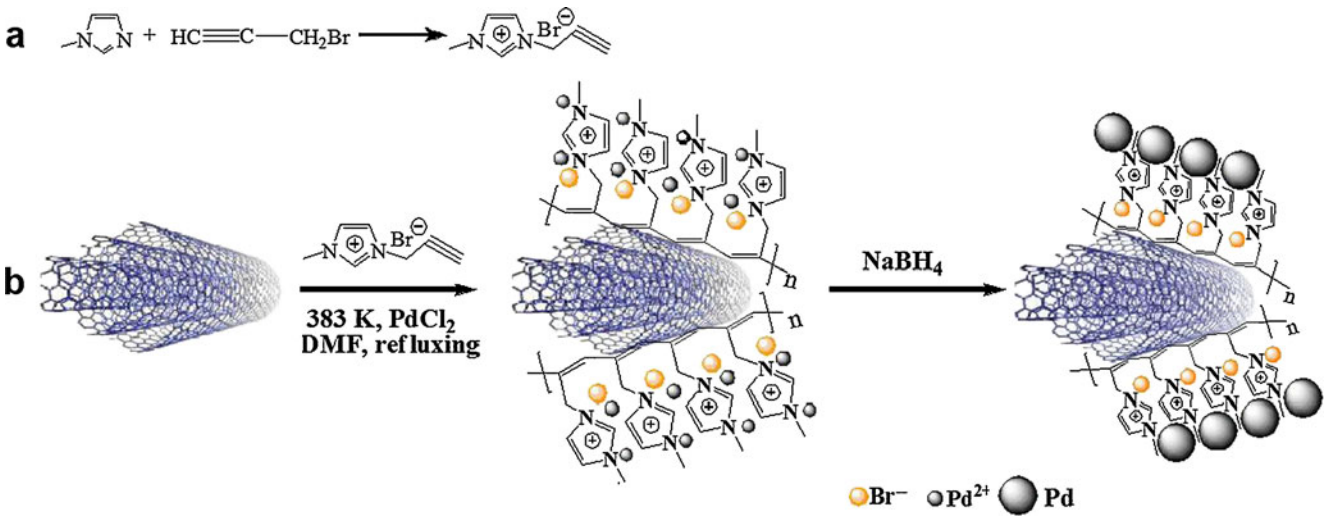

Fig. 1 Schematic diagram of the synthesis of [MPYI]Br (**a**) and one-pot synthesis procedure of the PdNPs-AILP-CNTs (**b**)

solution containing CNTs in the presence of $PdCl_2$ catalyst . Then, the solution of $NaBH_4$ was added dropwise to reduce Pd^{2+}, and the PdNPs-AILP-CNT nanohybrids were obtained in one pot.

The formation of PdNPs-AILP-CNT nanohybrids by the one-pot synthesis procedure is confirmed by FT-IR and thermal gravimetric analysis. Figure 2 shows the FT-IR spectra of MI, [MPYI]Br, and PdNPs-AILP-CNTs. Comparing the infrared spectrum of MI (curve a), the infrared spectrum of [MPYI]Br (curve b) obviously adds absorption peaks at 2,130 cm^{-1} (C≡C stretching vibration from C≡CH), 2,921 and 2,860 cm^{-1} (–C–H stretching vibration from $–CH_2$), and 1,168 cm^{-1} (imidazole ring stretching vibration); these indicate that the structure of the synthetic monomer is as expected (see Fig. 1a). The infrared spectrum of PdNPs-AILP-CNT nanohybrids (curve c) shows broad peaks centered at 3,448 cm^{-1} (=C–H stretching vibration), 1,643 and 1,566 cm^{-1} (C=C stretching doublet), 1,155 cm^{-1} (imidazole ring stretching vibration), and 875 cm^{-1} (C–H out-of-plane wagging vibration from $R_1R_2C=CHR_3$), consistent with the expected conjugated double bond structure of AILP. It should also be noted that the acetylene C≡C stretching band of the monomer at 2,130 cm^{-1} is absent in the spectrum of the PdNPs-AILP-CNTs, which implies the successful polymerization of [MPYI]Br.

Figure 3 shows the TGA results of PdNPs-AILP-CNT nanohybrids and CNTs in a nitrogen atmosphere. For CNTs, there is almost no weight loss in the measured temperature range of 298–850 K. However, for the PdNPs-AILP-CNTs, weight loss starts at about 473 K. In a nitrogen atmosphere, both PdNPs and CNTs in the PdNPs-AILP-CNT nanohybrids do not decompose below 850 K; the weight loss detected should come from the decomposition of AILP. The TGA results further confirm that the AILP were coated successfully onto the CNT surface. From the difference in weight loss between the CNTs and PdNPs-AILP-CNTs at 850 K, the amount of the surface-bound AILP on CNTs was estimated to be about 6 wt.% of the PdNPs-AILP-CNTs.

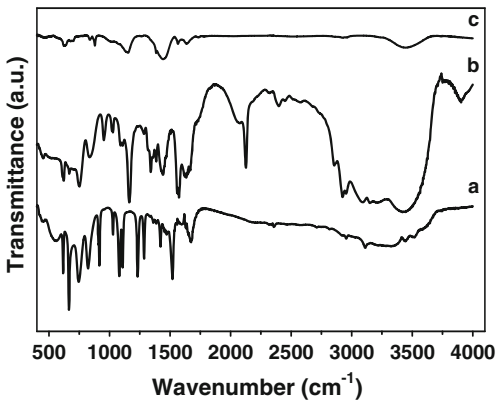

Fig. 2 The FT-IR spectra of MI (**a**), [MPYI]Br (**b**), and PdNPs-AILP-CNTs (**c**)

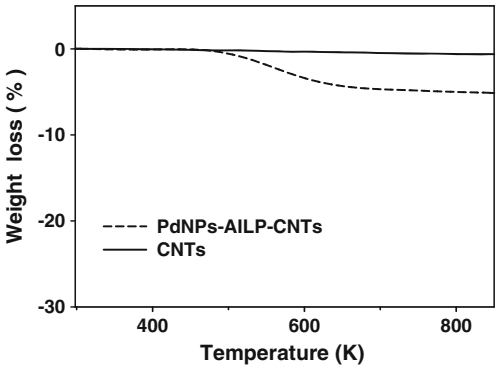

Fig. 3 The thermal gravimetric analysis of pristine CNTs and PdNPs-AILP-CNTs

The PdNPs in the PdNPs-AILP-CNT nanohybrids and PdNP-CNT nanocomposites were characterized by TEM, and the corresponding results are shown in Fig. 4a and b, respectively. From the insert plot in Fig. 4a, the AILP film on the CNT surface in PdNPs-AILP-CNTs can be observed clearly, and the thickness of the AILP film is about 2.5 nm. The size distribution was evaluated statistically through measuring the diameter of 100 PdNPs in the TEM images selected. For the PdNPs-AILP-CNT nanohybrids, it is noted that small PdNPs are uniformly deposited on the surface of CNTs-AILP without obvious aggregation (Fig. 4a) and have a narrow size distribution (2–6 nm) with an average diameter of about 3.5±0.5 nm (Fig. 4c). The dispersion of PdNPs in the PdNPs-AILP-CNT nanohybrids is better than that reported in the literatures [12, 13]. The related reasons may be as follows: (1) the imidazole groups in AILP not only serve as functionalization and dispersion agents to immobilize the Pd precursors through electrostatic interaction and coordination but also offer plentiful active sites for the nucleation and growth of PdNPs on the surface of CNTs [25], (2) the conjugated double bonds present in AILP seem to play an important role in PdNP stabilization and growth with a narrow size distribution [26]. However, for the PdNP-CNT nanocomposites, PdNPs appear as an obvious aggregation on the CNT surface (Fig. 4b), and the particle size was estimated roughly. A poor distribution between 5.8 and 18.4 nm with an average diameter of about 9.8±1.9 nm (Fig. 4d) was observed. It may be explained that PdNPs tend to deposit on those uneven defect sites of the CNTs, leading to poor dispersion and obvious aggregation, while being deposited on the CNTs.

On the other hand, Raman spectroscopy was also employed to investigate the structure changes of the CNTs, PdNPs-CNTs, PdNPs-AILP-CNTs, and CNTs-AO (refluxing CNTs in a mixed acid (H_2SO_4/HNO_3 in 1:3 *V*/*V* ratio)

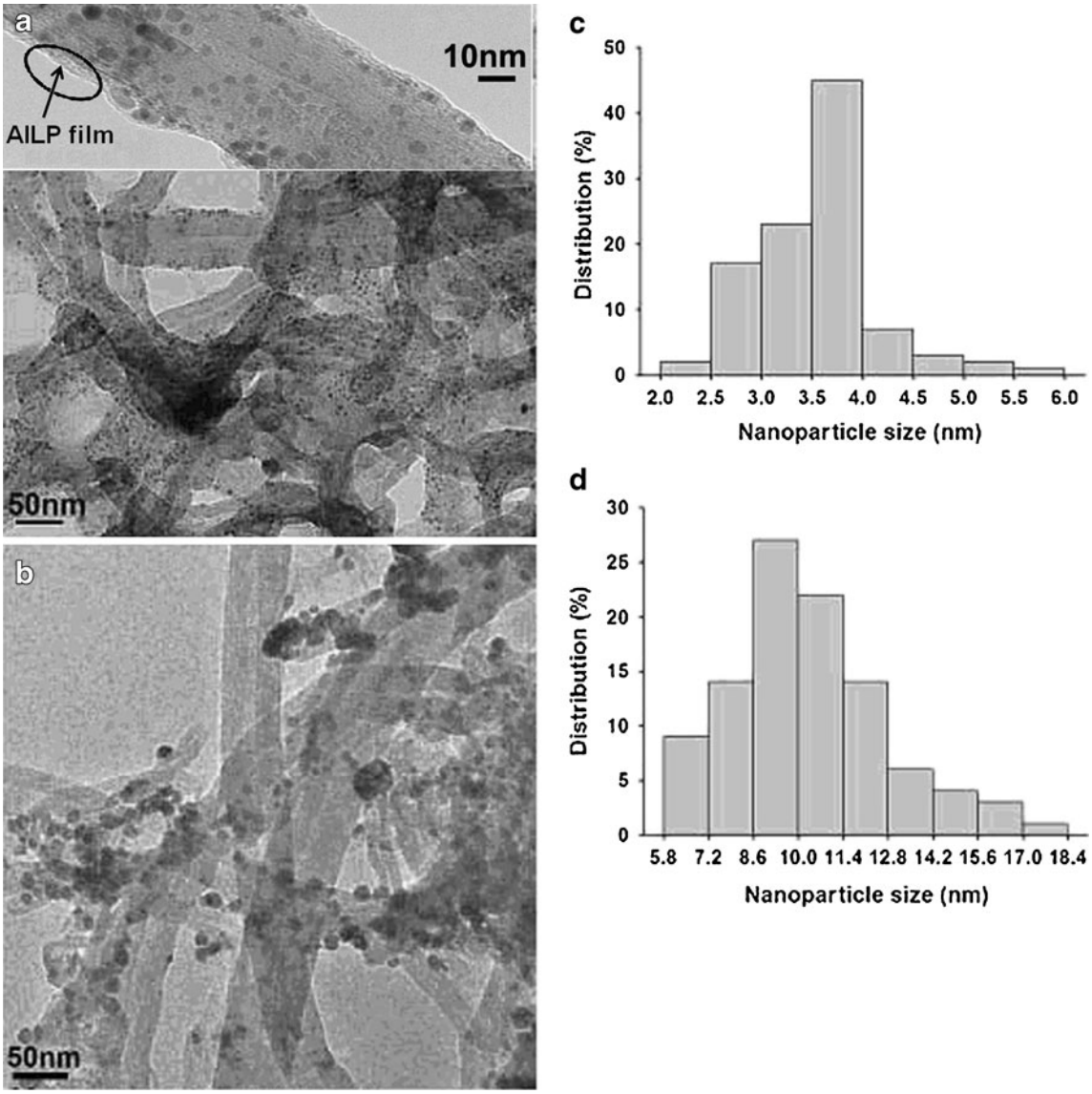

Fig. 4 The TEM images and size distribution diagrams of PdNPs -AILP-CNTs (**a**, **c**) and PdNPs-CNTs (**b**, **d**)

solution for 5 h), and the corresponding results are shown in Fig. 5. The peak at 1,320 cm^{-1} should be assigned to the A_{1g} breathing mode of a disordered graphitic structure (i.e., the D band), and the peak at ~1,570 cm^{-1} assigned to the E_{2g} structure mode of graphite (i.e., the G band). The G band reflects the structure of the sp^2-hybridized carbon atom. An additional side band at ~1,600 cm^{-1} was also observed, which was assigned as the D′ band. Both the D and the D′ bands are due to the defect sites in the hexagonal framework of graphitic materials [27]. The extent of the defects in graphitic materials can be quantified by the intensity ratio of the D to G bands (i.e., I_D/I_G). It can be obtained from Fig. 5 that the values of the I_D/I_G ratio are 1.39, 1.39, 1.45, and 1.60 for the CNTs, PdNPs-CNTs, PdNPs-AILP-CNTs, and CNTs-AO,

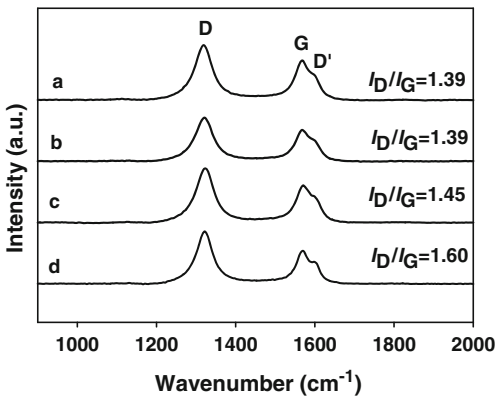

Fig. 5 The Raman spectra of the pristine CNTs (**a**), PdNPs-CNTs (**b**), PdNPs-AILP-CNTs (**c**), and CNTs-AO (**d**)

respectively. The equal I_D/I_G values between PdNPs-CNTs and CNTs suggest that deposition of PdNPs on the CNTs does not alter obviously the chemical structure of CNTs. It is noted that the values of I_D/I_G ratio of both PdNPs-AILP-CNTs and CNTs-AO are higher than that of the CNTs due to the surface modification process. However, the I_D/I_G ratio of PdNPs-AILP-CNTs is much lower than that of CNTs-AO. These indicate that noncovalent functionalization process of CNTs with AILP only changes the structure of CNTs slightly and causes less structural damage of CNTs than the typical acid-oxidized treatment, which will be beneficial in retaining the excellent physicochemical properties of CNTs (such as good electrical conductivity, chemical stability, and so on).

As mentioned above, the surface of CNTs modified with imidazolium ionic liquid polymers is of benefit to the high dispersion of metal nanoparticles on the CNTs [28]. However, the ionic liquid polymers used previously are usually insulative, which should be of no benefit to the electrochemical performance of electrocatalysts in fuel cells. Modification of CNTs with conductive ionic liquid polymer not only utilizes the advantages of ionic liquid polymer in the immobilization of metal nanoparticles but also solves the above problem. In order to show the difference in the electronic conductivities between conductive and non-conductive ionic liquid polymers, we prepared poly(1-vinyl-3-ethyl imidazolium bromide) functionalized CNTs (CNTs-PIL) and poly(1-methyl-3-(prop-2-ynyl)-imidazolium bromide) functionalized CNTs (CNTs-AILP) with the same weight percent of ionic liquid polymers (about 25 wt.%). The electronic conductivity of the CNTs-AILP film measured via the four-point method is around 3.1 Scm^{-1}, which is 4.5 times higher than that of the CNTs-PIL film (0.68 Scm^{-1}). The electrochemical impedance spectra of CNTs-AILP and CNTs-PIL films were also obtained to evaluate the charge transfer properties of the film (Fig. 6). Here, the Randles circuit (inset of Fig. 6) was chosen to fit the obtained impedance data. In the Randles circuit, it is assumed that the resistance of charge transfer (R_{ct}) and the diffusion impedance (Z_w) are both in parallel to the interfacial capacity (C_{dl}) [29]. R_l is the total Ohmic resistance of the system. The charge transfer term is observed as a deformed semicircle. After fitting the data of the deformed semicircles, the values of R_{ct} of the redox couples ($K_3Fe(CN)_6/K_4Fe(CN)_6$) are obtained according to the diameters of the fitted semicircles. The fitted R_{ct} value of CNTs-AILP is 57.1Ω, which is much smaller than that of CNTs-PIL (93.9Ω), indicating that the electron transfer rate on the electrochemical interface of CNTs-AILP is faster than that on CNTs-PIL.

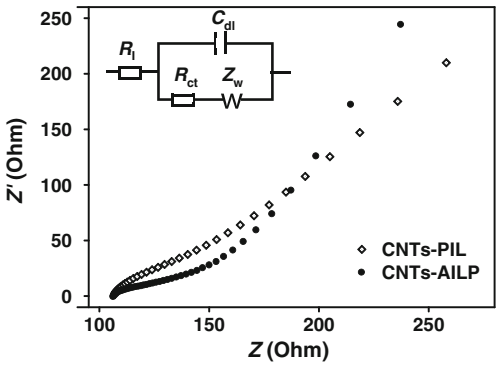

Fig. 6 EIS plots of CNTs-PIL, CNTs-AILP in 0.1 M KCl solution containing 2.5 mM $K_3Fe(CN)_6$ and 2.5 mM $K_4Fe(CN)_6$ obtained at a fixed potential of 0.2 V. The amplitude, 5 mV; frequency range, 0.1 Hz–1 MHz

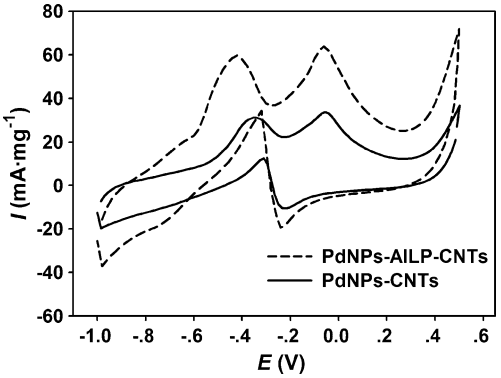

Fig. 7 Cyclic voltammograms recorded on the PdNPs-AILP-CNT and PdNPs-CNT electrocatalysts in nitrogen-saturated 0.1 M KOH+ 0.05 M glucose solution at a scan rate of 50 mV s^{-1}

Therefore, compared with PdNP-CNT nanocomposites, PdNPs-AILP-CNT nanohybrids have smaller PdNPs with a narrow size distribution and more uniform dispersion on the CNTs-AILP. Furthermore, there is less structural damage of CNTs and an acceptable electronic conductivity of AILP for the PdNPs-AILP-CNT nanohybrids. These imply that PdNPs-AILP-CNT nanohybrids should have good electrocatalytic properties for glucose oxidation.

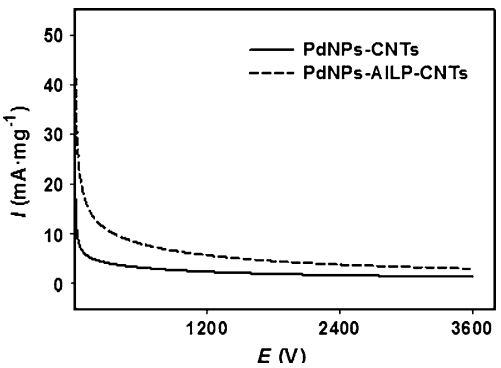

Fig. 8 Chronoamperometric curves of the PdNP-CNT and PdNPs-AILP-CNT electrocatalysts at a fixed potential of −0.1 V in nitrogen-saturated 0.1 M KOH+0.05 M glucose solution

Electrocatalytic properties of PdNPs-AILP-CNT nanohybrids for glucose oxidation

The performance of the PdNPs-AILP-CNTs and PdNPs-CNTs towards glucose electrooxidation was evaluated by cyclic voltammetry in 0.1 M KOH+0.05 M glucose solution. The results are shown in Fig. 7. The cyclic voltammograms of these two electrocatalysts have similar shape. There are two anodic peaks that are attributed to the oxidation of glucose in the positive scan. The first peak may be due to the dissociative adsorption of glucose on Pd to produce adsorbed intermediates by dehydrogenation [30, 31]. The second anodic peak likely corresponds to the complete oxidation of glucose after the poisoning intermediates on the electrocatalyst surface are moved by the OH_{ad} radicals formed by the partial discharge of OH^- under the upper potential region [30, 31]. From Fig. 7, it is noted that the onset potential (−0.59 V) and the first anodic peak potential (−0.42 V) of the glucose oxidation on Pd NPs-AILP-CNTs shift negatively, compared with those on the PdNPs-CNTs (−0.50 V for the onset potential and −0.36 V for the first anodic peak potential). Considering that the imidazolium ring moieties of the AILP might interact with the π-electronic nanotube surface by virtue of cation-π and/or π–π interactions, the close contact between CNTs and Pd NPs via AILP as a linker probably contributes to high electron transfer between CNTs and PdNPs [29]. Furthermore, the mass activity of PdNPs-AILP-CNTs at the first anodic peak potential (57 mA mg^{-1} at −0.42 V) is much higher than that of the PdNPs-CNTs (31 mA mg^{-1} at −0.36 V), most likely due to the smaller sizes and higher dispersion of PdNPs in the PdNPs-AILP-CNT catalyst.

Due to the importance in practical application, the electrochemical stabilities of these two electrocatalysts for glucose oxidation were investigated by chronoamperometric technique, a useful method for the evaluation of the electrocatalysts. Figure 8 shows the current–time curves of the PdNPs-AILP-CNTs and PdNP-CNT electrocatalysts recorded at −0.10 V. It is noted that the current density at 3,600 s at the PdNPs-AILP-CNT nanohybrids (3 mA mg^{-1}) is 2.2 times than that at the PdNP-CNT nanohybrids (1 mA mg^{-1}). This implies that the PdNPs-AILP-CNT electrocatalyst has higher electrocatalytic activity and better electrochemical stability toward glucose oxidation than PdNP-CNT nanohybrid [32]. The above results also imply that the applications of the PdNPs-AILP-CNT nanohybrids could be extended to direct alcohol fuel cells and biosensors.

Conclusions

We have developed a facile procedure to disperse PdNPs on CNTs via the in situ polymerization of acetylenic ionic liquid monomers catalyzed by $PdCl_2$ on CNTs and the following reduction of $PdCl_2$ with $NaBH_4$ in one pot. As the result of the uniform distribution of the surface functional groups provided by AILP and the acceptable electronic conductivity of the AILP layer, PdNPs supported on the CNTs-AILP have a smaller particle size and better dispersion than those on CNTs without AILP modification. The PdNPs-AILP-CNT electrocatalyst shows better performance for the electrooxidation of glucose than the PdNP-CNT electrocatalyst. The strategy developed in this paper could be extended to the preparation of other CNT-supported metal nanoparticle electrocatalysts which are used widely in fuel cells and biosensors.

Acknowledgments This work is supported by the NSFC (20975033, 20905024), the Program for Changjiang Scholars and Innovative Research Team in University (PCSIRT), and the National Basic Research Program of China (no. 2009CB421601).

References

1. Lim SH, Wei J, Lin JY, Li QT, You JK (2005) Biosens Bioelectron 20:2341–2346
2. Bianchini C, Shen PK (2009) Chem Rev 109:4183–4206
3. Baughman RH, Zakhidov AA, Heer WA (2002) Science 297:787–792
4. Meng L, Jin J, Yang GX, Lu TH, Zhang H, Cai CX (2009) Anal Chem 81:7271–7280
5. Liu B, Li HY, Die L, Zhang XH, Fan Z, Chen JH (2009) J Power Sources 186:62–66
6. Hu FP, Shen PK, Li YL, Liang JY, Wu J, Bao QL, Li CM, Wei ZD (2008) Fuel Cells 8:429–435
7. Sun ZP, Zhang XG, Liu RL, Liang YY, Li HL (2008) J Power Sources 185:801–806
8. Tian ZQ, Jiang SP, Liang YM, Shen PK (2006) J Phys Chem B 110:5343–5350
9. Xue B, Chen P, Hong Q, Lin J, Tan KL (2001) J Mater Chem 11:2378–2381
10. Choi HC, Shim M, Bangsaruntip S, Dai H (2002) J Am Chem Soc 124:9058–9059
11. Yoon B, Wai CM (2005) J Am Chem Soc 127:17174–17175
12. Ye XR, Lin Y, Wai CM (2003) Chem Commun 9:642–643
13. Chen X, Hou Y, Wang H, Cao Y, He J (2008) J Phys Chem C 112:8172–8176
14. Karousis N, Tsotsou GE, Evangelista F, Rudolf P, Ragoussis N, Tagmatarchis N (2008) J Phys Chem C 112:13463–13469
15. Bera D, Kuiry SC, McCutchen M, Kruize A, Heinrich H, Meyyappan M, Seal S (2004) Chem Phys Lett 386:364–368
16. Kim KS, Choi S, Cha JH, Yeon SH, Lee HJ (2006) J Mater Chem 16:1315–1317
17. Migowski P, Dupont J (2006) Chem Eur J 13:32–39
18. Scheeren CW, Machado G, Teixeira SR, Morais J, Domingos JB, Dupont J (2006) J Phys Chem B 110:13011–13020
19. Zhao DB, Fei ZF, Ang WH, Dyson PJ (2006) Small 2:879–883
20. Batra D, Seifert S, Varela LM, Liu ACY, Firestone MA (2007) Adv Funct Mater 17:1279–1287
21. Wu BH, Hu D, Kuang YJ, Liu B, Zhang XH, Chen JH (2009) Angew Chem Int Ed 48:4751–4754

22. Schottenberger H, Wurst K, Horvath UEI, Cronje S, Lukasser J, Polin J, McKenzie JM, Raubenheimer HG (2003) Dalton Trans 22:4275–4278
23. Delts W, Cukor P, Rubner M, Jopson H (1981) Ind Eng Chem Prod Res Dev 20:696–704
24. Marcilla R, Bleazquez JA, Rodriguez J, Pomposo JA, Mecerreyes D (2004) J Polym Sci, A: Polym Chem 42:208–212
25. Park HS, Choi BG, Yang SH, Shin WH, Kang JK, Jung DH, Hong WH (2009) Small 5:1754–1760
26. Mazumder V, Sun S (2009) J Am Chem Soc 131:4588–4589
27. Hsin YL, Hwang KC, Yeh CT (2007) J Am Chem Soc 129:9999–10010
28. Fukushima T, Aida T (2007) Chem Eur J 13:5048–5058
29. Guo SJ, Dong SJ, Wang EK (2009) Adv Mater 21:1–4
30. Nirmala Grace A, Pandian K (2007) J Phys Chem Solids 68:2278–2285
31. Aoun SB, Dursun Z, Koga T, Bang GS, Sotomura T, Taniguchi I (2004) J Electroanal Chem 567:175–183
32. Wang RF, Liao SJ, Ji S (2008) J Power Sources 180:205–208